Bound states of two-dimensional solitons in the discrete nonlinear Schrödinger equation

2001 J. Phys. A: Math. Gen. 34 9615

(http://iopscience.iop.org/0305-4470/34/45/302)

INSTITUTE OF PHYSICS PUBLISHING JOURNAL OF PHYSICS A: MATHEMATICAL AND GENERAL

J. Phys. A: Math. Gen. **34** (2001) 9615–9629 PII: S0305-4470(01)23896-7

Bound states of two-dimensional solitons in the discrete nonlinear Schrödinger equation

P G Kevrekidis[1,2], **B A Malomed**[3] **and A R Bishop**[1]

[1] Theoretical Division and Center for Nonlinear Studies, Los Alamos National Laboratory, Los Alamos, NM 87545, USA
[2] Department of Mathematics and Statistics, University of Massachusetts, Lederle Graduate Research Tower, Amherst, MA 01003-4515, USA
[3] Department of Interdisciplinary Studies, Faculty of Engineering, Tel Aviv University, Tel Aviv, Israel

Received 5 April 2001, in final form 4 September 2001
Published 2 November 2001
Online at stacks.iop.org/JPhysA/34/9615

Abstract

The existence and stability of bound states (BSs) of solitary excitations in the two-dimensional discrete nonlinear Schrödinger lattice are considered. Stable BSs of two or three solitons are categorized according to their vorticity S ($S = 0$ corresponds to ordinary pulses, while $S = 1$ corresponds to discrete vortex solitons). Interactions of $S = 0$ solitons are found to have clear particle-like characteristics, which can be very accurately predicted in the framework of the perturbation theory that we develop. Triangular bound states of three solitons are also constructed, and particle-like characteristics in their behaviour are followed in numerical experiments. Finally, stable bound states of two vortex solitons, and $S = 0$–1 stable complexes are constructed. For the latter state, we find a weak dependence of the interaction-generated stability eigenvalue on the distance between the two solitons.

PACS numbers: 05.45.Yv, 05.50.+q, 03.65.−w

1. Introduction

The discrete nonlinear Schrödinger (DNLS) equation is a benchmark system for studies of dynamics in Hamiltonian nonlinear lattice models. Physical realizations of such systems include local denaturation of the DNA double strand [1], materials in glassy states [2], complex electronic materials [3], as well as bundles of optical fibres or waveguides [4–7].

Recent experimental work [3, 8–10] has greatly increased the interest in these systems, stimulating theoretical efforts aimed at understanding the behaviour of basic models of the DNLS type. An issue of particular interest is the possibility of energy trapping and localization in *intrinsic localized modes* (ILMs), which are also referred to as *discrete breathers* [11].

0305-4470/01/459615+15$30.00

Even though some theoretical methods and results concerning ILMs apply to multidimensional lattices (e.g., their proof of existence in [12]), most theoretical techniques have been developed for treating the problem in one dimension (1D). Nevertheless, a few numerical and analytical works targeted 2D nonlinear lattices of the Fermi–Pasta–Ulam (FPU) [13, 14], Klein–Gordon (KG) [15, 16], and DNLS [17–24] types. Some systems in 3D were also considered [25].

In this work, we aim to explore an aspect of higher- (in particular, two-) dimensional lattice dynamics that was not examined in these previous works, namely, a possibility of formation of stable multi-soliton bound states (BSs). In part, this extends the work initiated in [19, 26], which addresses the construction and stability of solitary excitations in multi-dimensional nonlinear lattices, as well as recent work on multiple-pulse bound states in 1D lattices [27, 28]. The study will involve both an analytical approach via the soliton perturbation theory, and numerical simulations of the formation and stability of multi-soliton BSs.

The study of this problem in the framework of the DNLS model is suggested by its ubiquity in applications. However, the general results obtained below are expected to be valid for nonlinear KG lattices too—at least, within the spatial and temporal scales for which the KG lattice equations may be approximated by the corresponding DNLS envelope equations [29]. This is true for the KG lattices with soft nonlinearities, for which general dynamical features have been shown (see, e.g., [30, 31]) to be the same as in the envelope equations, including interactions between solitons and between solitons and lattice phonons.

For KG lattices with hard nonlinearities and/or FPU chains, such extensions are not *a priori* obvious, and should be justified by detailed numerical comparisons. In particular, the interactions between solitons and lattice phonons in the models of the latter class are different from those in DNLS systems [30].

The solitary pulses whose bound states are considered in this work include ordinary localized 2D pulses, which we call $S = 0$ solitons, and *discrete localized vortices* (which will be called $S = 1$ solitons, S standing for the soliton's 'spin'). The latter ones were originally discussed in [12, 32], and then constructed for KG [16] and DNLS [24] lattices, and identified as stable objects in the case of very strong discreteness. Recently, these modes were revisited in [26], where a detailed stability analysis has been performed.

The paper is structured as follows: in sections 2 and 3, analytical and numerical results for BSs of $S = 0$ solitons are presented. In section 4, bound complexes of $S = 0$ with $S = 1$ solitons, as well as BSs of $S = 1$ solitons, are considered. Only numerical results are given for the latter types of BSs, which are found far from the continuum limit, where the validity of the perturbation theory is questionable.

2. Bound states of zero-spin solitons: analytical considerations

2.1. The model

The 2D DNLS equation is

$$\mathrm{i}\dot{u}_{m,n} + C\Delta_2 u_{m,n} + |u_{m,n}|^2 u_{m,n} = 0 \tag{2.1}$$

where $C = 1/h^2$ is the coupling constant (h is the lattice spacing), and $\Delta_2 u_{m,n} = u_{m+1,n} + u_{m,n+1} + u_{m,n-1} + u_{m-1,n} - 4u_{m,n}$ is the 2D discrete Laplacian. As in the 1D case [27], the consideration of the BS problem makes it necessary to have analytical approximations for its two ingredients: a potential of interaction between two solitons, and the (*Peierls–Nabarro*) potential of the interaction of a single soliton with the underlying lattice. In practical terms, this necessity largely restricts us to the quasi-continuum approximation (i.e. to the case of wide solitons).

In comparison with the 1D case [27], there exist two additional problems: an exact form of the 2D soliton in the continuum NLS model is not known, and this soliton is unstable against *weak collapse* [21]. The latter problem may be ignored, tacitly assuming that, in fact, we will be dealing with a 'sufficiently discrete' soliton, for which the collapse is already removed by the discrete character of the model. As concerns the lack of the exact shape of the 2D soliton in the continuum model, we will use a variational approximation (VA) for it. In fact, we will need *three* different versions of VA, as described below.

2.2. The quasi-continuum variational approximation

Generally, a soliton is sought as a stationary solution,

$$u_{m,n}(t) = U_{m,n}\mathrm{e}^{-\mathrm{i}\Lambda t} \tag{2.2}$$

where the real amplitudes $U_{m,n}$ satisfy an equation

$$\Lambda U_{m,n} + C\Delta_2 U_{m,n} + U_{m,n}^3 = 0 \tag{2.3}$$

and the coupling constant $C \equiv h^{-2}$ is determined by the lattice spacing h. Notice that one of the two parameters in equation (2.3) can be scaled out; nevertheless, we keep both of them, as it helps to understand in detail the approach to the continuum limit ($h \to 0$).

The frequency Λ parametrizes a family of solitons, and it is easy to understand that solitons exist only if Λ is *negative*. The continuum limit for equation (2.3) is

$$\Lambda U + U'' + r^{-1}U' + U^3 = 0 \tag{2.4}$$

where the prime stands for $\mathrm{d}/\mathrm{d}r$, $r = h\sqrt{m^2+n^2}$ being the radial spatial coordinate.

The simplest version of VA for the continuum-limit equation (2.4) is based on the *ansatz*

$$U = A\mathrm{e}^{-\kappa r}. \tag{2.5}$$

It is straightforward to find the following result produced by this version of VA:

$$A^2 = -8\Lambda \qquad \kappa^2 = -\Lambda. \tag{2.6}$$

Note that a somewhat similar ansatz, $U_{m,n} = A\exp\left[-\kappa\left(|m|+|n|\right)\right]$, may be applied directly to the discrete equation (2.3). However, unlike the ansatz (2.5) in the continuum model, the latter one gives rise to much more cumbersome results than (2.6), so we will not pursue this possibility below.

As a matter of fact, the ansatz (2.5) is *not* sufficient to produce a consistent approximation for the potential of the interaction between two widely separated solitons even in the continuum model, because the correct asymptotic form of a solution to equation (2.4) at $r \to \infty$ is, as it is well known,

$$U \approx Br^{-1/2}\mathrm{e}^{-\kappa r} \tag{2.7}$$

with some constant B. From the comparison with equation (2.7) it is obvious that the pre-exponential multiplier $r^{-1/2}$ is missing in the ansatz (2.5) if one is going to use it as an asymptotic expression at $r \to \infty$. To fix this inconsistency, one may try to use a more sophisticated ansatz, for instance,

$$U = B\left(r_0 + r\right)^{-1/2}\exp\left(-\kappa r\right) \tag{2.8}$$

with an extra variational parameter r_0. However, this ansatz is not analytically tractable. Therefore, we will postulate that the amplitude B in the asymptotic expression (2.7) is related to A from equation (2.5) as follows:

$$B = c\kappa^{-1/2}A \tag{2.9}$$

where c is a 'phenomenological' numerical constant, while the multiplier $\kappa^{-1/2}$ is added here to provide for the correct dimension of the amplitudes.

A correct calculation of the potential of the interaction between an isolated soliton and the underlying lattice demands an ansatz different from both ones (2.5) or (2.8), as they have a cusp at $r = 0$, which would be a major drawback in the consideration of the soliton–lattice interaction. To remove the artificial cusp, one can introduce an ansatz $A\ \mathrm{sech}(\kappa r)$, cf the expression (2.5); however, the latter one is intractable. Therefore, the only practical possibility to address the soliton–lattice interaction is to use the Gaussian ansatz,

$$U = \alpha \exp(-\mu r^2). \tag{2.10}$$

An easy VA-based calculation then yields

$$\alpha^2 = -4\Lambda \qquad \mu = -2\Lambda \tag{2.11}$$

(recall that $\Lambda < 0$). Of course, the Gaussian ansatz has a wrong asymptotic form at $r \to \infty$, but this feature is not crucial for the soliton–lattice interaction, unlike the interaction between two solitons.

2.3. The potentials of the soliton–soliton and soliton–lattice interactions

2.3.1. The soliton–soliton interaction. The interaction between widely separated solitons is determined by their asymptotic forms. Once we adopt the form (2.7), it is possible to apply a general method for the derivation of the interaction potential developed (for two- and three-dimensional solitons) in [33]. The final expression for the interaction potential is

$$U_{\mathrm{int}}(L, \phi) = -2B^2\sqrt{2\pi\kappa/L}\ \exp(-\kappa L)\cos\phi \tag{2.12}$$

where B and κ have exactly the same meaning as in the asymptotic expression (2.7), while L and ϕ are the separation and phase difference between the centres of two identical solitons (i.e. those having the same amplitude B in the expression (2.7)). We stress that the expression (2.12) is correct irrespective of the correctness of the various versions of VA for an isolated soliton.

Using the interaction potential (2.12) and taking into account the kinetic part of the underlying Lagrangian, one can derive dynamical equations governing the interaction of two widely separated solitons. First of all, it is possible to derive an evolution equation for the relative phase ϕ. After simple manipulations, it takes the form

$$\ddot{\phi} = (c^2/2)A^2\sqrt{\kappa/(2\pi L)}\exp(-\kappa L)\sin\phi \tag{2.13}$$

where c is the same positive constant as in equation (2.9), and the overdots stand for time derivatives. From equation (2.13) it immediately follows that only the bound state with the phase difference $\phi = \pi$ may be stable, which is the same conclusion as in the 1D case [27].

After fixing this value of ϕ, the interaction potential (2.12), as a function of the separation L, becomes

$$U_{\mathrm{int}}(L) = 2B^2\sqrt{2\pi\kappa/L}\ \exp(-\kappa L) \tag{2.14}$$

which corresponds to repulsion between the two solitons.

2.3.2. The soliton–lattice interaction. The potential of the interaction of the quasi-continuum 2D soliton with the underlying lattice can be calculated in essentially the same way as in [27] for the 1D case. As mentioned above, to do it one should use the Gaussian version of VA based on equations (2.10) and (2.11) (if, instead, one tries to use the approximation of the type (2.5) with a cusp at $r = 0$, the result will be that the interaction potential is *not* exponentially small in the quasi-continuum limit $h \to 0$, which is definitely incorrect).

Thus, using the Gaussian ansatz, and assuming that the soliton's centre is located at a point with coordinates (η, ξ), an eventual expression for the soliton–lattice interaction can be obtained in the following form:

$$U_{\rm latt}(\eta,\xi) = -2\pi|\Lambda|\exp\left(-\frac{\pi^2}{8|\Lambda|h^2}\right)\left[\cos\left(\frac{2\pi}{h}\eta\right)+\cos\left(\frac{2\pi}{h}\xi\right)\right] \quad (2.15)$$

which contains the natural exponential smallness in the lattice spacing h.

2.4. The final result

The minimum possible distance $L_{\rm min}$ between the solitons in a stable stationary quasi-continuum state can be found from the balance condition for the repulsion force generated by the potential (2.12) and pinning force generated by the potential (2.15). Using the fact that both potentials are exponentially small, in the lowest approximation we can easily find

$$L_{\rm min} \approx \pi^2/\left(8|\Lambda|^{3/2}h^2\right). \quad (2.16)$$

An additional remark is that the smallest separation between two solitons is realized if the vector connecting their centres is parallel to the *diagonal* of the underlying square lattice.

Thus, it is possible to develop the asymptotic description of the bound states of two 2D $S = 0$ solitons at essentially the same level as in the 1D case [27]. A simple estimate for the maximum possible value of $L_{\rm min}$, using data from [19], shows that this value is typically (for lattice spacings for which single pulses exist) of the order of a few lattice spacings. However, in that case, the pulses are not well separated anymore, and the estimate is not reliable. This statement agrees with our finding that, for typical values of h, well-separated pulse pairs were always found to exist as solutions of the 2D DNLS equation. For very small separations between the pulses, 2D generalizations of *twisted* localized modes (see [26, 34–38]) exist, see below. The existence and stability ranges for these modes were considered in detail (for two dimensions) in [26, 38].

3. Bound states of zero-spin solitons: numerical results

The remark given at the end of the previous section will be quite helpful in understanding results presented in this section for BSs constructed by the concatenation of two or three zero-vorticity pulses. To create such states, we solve equations (2.3) on a lattice of a size $N \times N$ with an initial guess in the form of a two-soliton state, taken as suggested by the analytical results presented above. Typically, in our computations N varied between 20 and 40, which turns out to be quite sufficient for the comprehensive study of the bound states. We subsequently solved equations (2.3) by means of Newton iteration until a convergence criterion was met (which most commonly required that the L^2 norm of the error was smaller than a tolerance $\sim 10^{-8}$). An alternative method for the solution of the equations was used in [19].

Once a stationary solution $U_{m,n}$ had been identified, numerical linear analysis of its stability was performed. This was done by substituting $u_{m,n} = \exp(-{\rm i}\Lambda t)(U_{m,n} + \epsilon v_{m,n})$ into equation (2.1), which yields the linearized equation (see, e.g., [39, 40])

$${\rm i}\dot{v}_{m,n} + C\Delta_2 v_{m,n} + 2|U_{m,n}|^2 v_{m,n} + U_{m,n}^2 v_{m,n}^* + \Lambda v_{m,n} = 0 \quad (3.17)$$

the asterisk standing for the complex conjugation. Further, the substitution of $v_{m,n} = a_{m,n}\exp(-{\rm i}\lambda t) + b_{m,n}\exp({\rm i}\lambda^\star t)$ into equation (3.17) leads to an eigenvalue problem for the stability exponent λ, based on the stationary equations

$$\lambda a_{m,n} = -C\Delta_2 a_{m,n} - 2|U_{m,n}|^2 a_{m,n} + \Lambda a_{m,n} - U_{m,n}^2 b_{m,n}^\star \quad (3.18)$$

$$-\lambda b_{m,n}^\star = -C\Delta_2 b_{m,n}^\star - 2|U_{m,n}|^2 b_{m,n}^\star + \Lambda b_{m,n}^\star - (U^*_{m,n})^2 a_{m,n}. \quad (3.19)$$

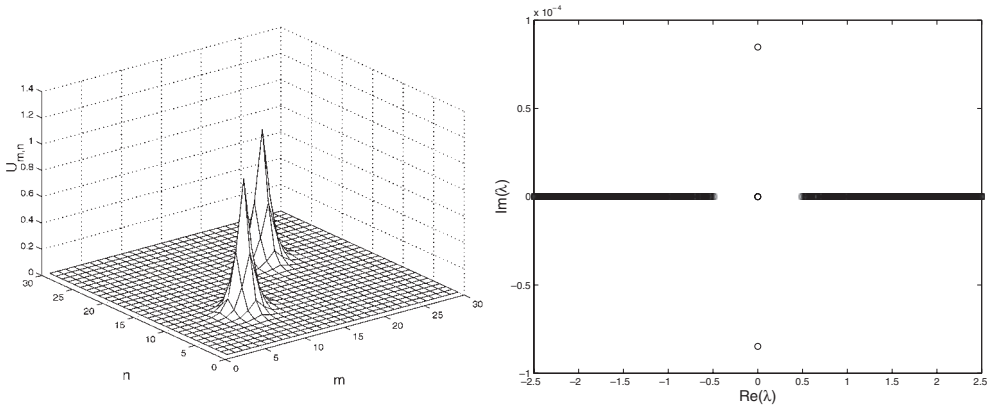

Figure 1. The left and right panels show an unstable pulse configuration with zero phase difference between two-dimensional pulses, and the spectrum of its eigenvalues, as produced by numerical calculations at $\Lambda = -0.5$ and $C = 0.25$. The presence of an (interaction-generated) pair of imaginary eigenvalues signals the presence of the instability.

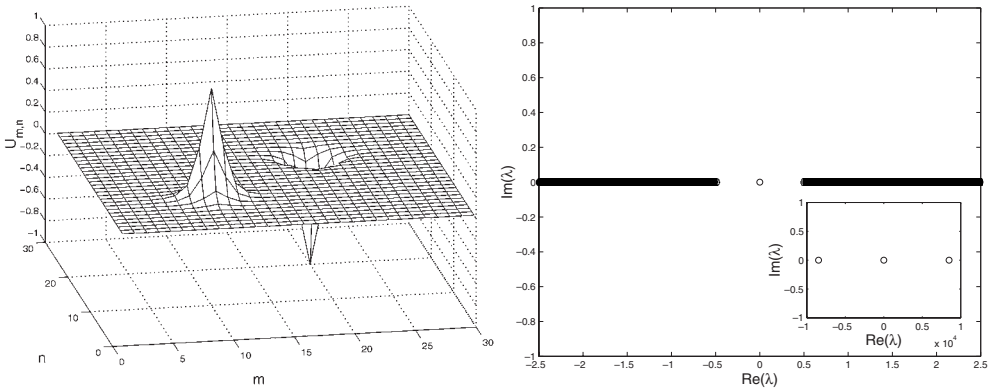

Figure 2. The same as in figure 1, but for a stable configuration with π phase difference between the pulses. The inset is a blowup in the vicinity of the origin of the spectral plane, which demonstrates the true stability of this bound state.

Obviously, real eigenvalues λ correspond to neutrally stable oscillatory eigenmodes, while the presence of eigenvalues with $\mathrm{Im}\,\lambda \neq 0$ signals an instability. Due to the Hamiltonian nature of the system, $\lambda^\star$, $-\lambda$, $-\lambda^\star$ are also eigenvalues if λ is an eigenvalue.

We now turn to the presentation of numerical results. We have found that BSs with the zero phase difference between two identical solitons *always* possess an unstable eigenvalue that renders such complexes unstable. An example of this is shown in figure 1, where the left panel shows the configuration which is a solution of equations (2.3), while the right panel shows the corresponding set of the eigenvalues λ, where it can be clearly seen that the interaction eigenvalue is unstable (imaginary). In contrast, for pulses with the opposite 'parity' (i.e. with a phase difference π between them), we observe in figure 2 that the interaction eigenvalues are stable (see, in particular, the inset in the right panel of figure 2). Such a stable 'up–down' configuration is shown in the left panel of figure 2. These results comply with their 1D counterparts (see i.e. [27]), as well as with what is predicted by the 2D VA developed in the previous section.

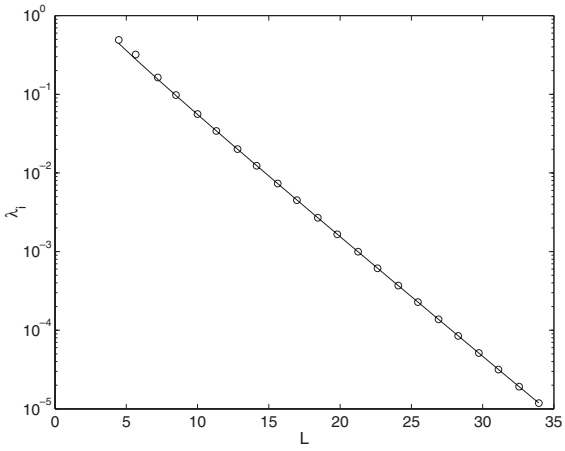

Figure 3. The interaction-induced eigenvalue for a bound state of two pulses with π phase difference versus the distance L between them, for $\Lambda = -0.5$, $C = 0.25$. The numerical-data points are shown by circles, while the least-squares fit described in the text is depicted by the solid line. Notice the deviation from the least-squares fit (which, in fact, is very close to the theoretical prediction) at very small values of L, where the theory is no longer valid (see text).

One might worry about a possibility of collisions of the interaction-generated eigenvalues with other ones, which could lead to oscillatory instabilities [37,41,42]. However, as it was argued in [28], the condition $L > L_{\min}$ precludes collisions between the interaction eigenvalues and translational ones (those which correspond to the breaking of the translational invariance). We have concluded that this condition is typically not very stringent. On the other hand, for very discrete cases, an additional possibility is a collision with eigenvalues that are at the edge (or have just bifurcated from the edge) of the continuous spectrum. A criterion for the avoidance of collisions of the latter type is $\sqrt{U_{\rm int}} < |\Lambda|$ (since the edge of the continuous spectrum is at $\Lambda = |\Lambda|$). It has been found for 1D problems [28,43], and also for 2D in [26,38], that such collisions with the band edge are *only* possible for twisted-like modes for which the 'pulse separation' is one or, maximum, two lattice sites. In fact, in the latter case, one cannot really speak of separated pulses. Hence, in the cases of well-separated pulses considered herein, such collisions do not occur, and the configuration is linearly stable for *any* relevant value of the lattice spacing.

To further test the predictions of the perturbation theory based on the VA, we computed the interaction-generated eigenvalue λ_i versus the distance between the pulses. Results are shown in figure 3 for $\Lambda = -0.5$ and $C = 0.25$ (although the validity of the conclusions was also tested for other parameter values). It is easy to show, using the results from the previous section, that the interaction eigenvalue can be estimated as follows:

$$\lambda_i \sim \sqrt{U_{\rm int}} \sim L^{-1/4} \exp(-\kappa L/2) \tag{3.20}$$

where $U_{\rm int}$ is the interaction potential (2.14). The least-squares fit of a curve $\lambda_i = ar^{-b}\exp(-cr)$, shown by the solid line in figure 3, to the numerically found values of λ_i yields $b = 0.247\,889$ and $c = 0.340\,191$, which are fairly close to the analytically predicted values $b = 0.25$ and $c = 0.353\,553$ in equation (3.20), small discrepancies being well justifiable by the generally approximate and, and, in particular, quasi-continuum nature of the analytical calculation, and, in a part, also by details of the numerical computations (such as, for instance, the effect of domain boundaries).

A principal conclusion suggested by the above results is the particle-like character of the interaction between the pulses even in the regime of strong discreteness (notice that $C = 0.25$ corresponds to the lattice spacing $h \equiv C^{-1/2} = 2$). The validity of equation (3.20) (and hence of equation (2.14) in section 2) has been verified for different values of the lattice spacing. An analogous feature, namely, slightly different but still particle-like behaviour of the interaction in the 1D DNLS, has been discussed in section 4 of [27].

For small distances L between the two pulses, the theoretical prediction is expected to break down as is observed for small L in figure 3. This is due to the fact that the interaction eigenvalues become of the same order of magnitude as the translational ones, hence they interact and, eventually (with the decrease of L) collide, giving rise to quartets of eigenvalues that bear oscillatory instabilities, as mentioned above. Notice that for the two left-most points of the graph in figure 3 the configuration is unstable due to the appearance of such a Hamiltonian Hopf bifurcation.

Typically, we have found that deviations from the variational prediction (due to the interaction between different eigenvalues) begin to occur for the ratio $L/L_{\min}$ taking values, typically, between 1 and 10. For instance, in the case shown in figure 3, these deviations start to occur for $L/L_{\min} \approx 8$.

We have also tested the validity of equation (2.15). This was done by fixing $|\Lambda| = 1$ and probing the energy of the soliton–lattice interaction as a function of the coupling constant. The energy was measured by computing the energy of a stable steady state (a pulse whose centre is placed on-site in both directions) and subtracting the energy of an unstable steady state (the pulse centred between sites in both directions [19]). We have found that for $h < 0.9$, the approach to the continuum limit (in which collapse effects appear) deteriorates agreement between the theoretical and numerical results. Similarly, for $h > 2$, the lattice becomes very discrete and the quasi-continuum approximation for the solution no longer is a good one. For $0.9 < h < 2$, we have numerically tested the agreement, using, as a measure for the quantitative comparison, the absolute value of the slope of the (semilog) plot of the soliton–lattice interaction energy versus the coupling constant C. For $|\Lambda| = 1$, this slope should be, according to equation (2.15), $s \approx 1.2337$. Numerically, we have found $s \approx 1.2436$, hence the relative error is $\approx$0.008. We thus conclude that the quasi-continuum approximation gives very good agreement with the numerical results in the range of $0.9 < h < 2$.

However, features indicating discreteness effects, if compared to the quasi-continuum approximation, are visible too. One of them is a bifurcation of two intrinsic modes of the solitary wave from the edge of the continuum spectrum. Such bifurcations have been identified as arising from the discreteness acting as a singular perturbation added to the continuum model in [44–48]. Exponential, as well as power-law, dependences of the bifurcation effects on the lattice spacing have been assessed in those works. In figure 4, we numerically monitor the variation of the two eigenvalues bifurcating from the band edge—not versus the lattice spacing, but rather as a function of the separation between individual pulses that form the BS. Our numerical results indicate that:

- As the pulse separation increases (i.e. as the state gradually goes over into a pair of noninteracting pulses), the two eigenvalues approach an asymptotic value for isolated pulses, which depends solely on the lattice spacing (as predicted in the above-mentioned works).
- However, as the separation between the two individual pulses decreases, an effect of the interaction shows itself in the opposite variation of the two eigenvalues, eventually driving one of them back into the phonon band. It should be noted here that after returning to the phonon band, these eigenvalues will no longer pertain to localized modes. It is clear that since these eigenvalues bifurcated from the continuous spectrum, they bear the *Krein signature* of the continuous-spectrum eigenvalues (see, e.g., [27, 32, 49] and references therein for an explanation of the Krein signature and its relevance). Hence, upon collision with the continuous-spectrum eigenvalues (when the former return to the band), the eigenvalues will just go through each other [27] and *no oscillatory instability will be present*.

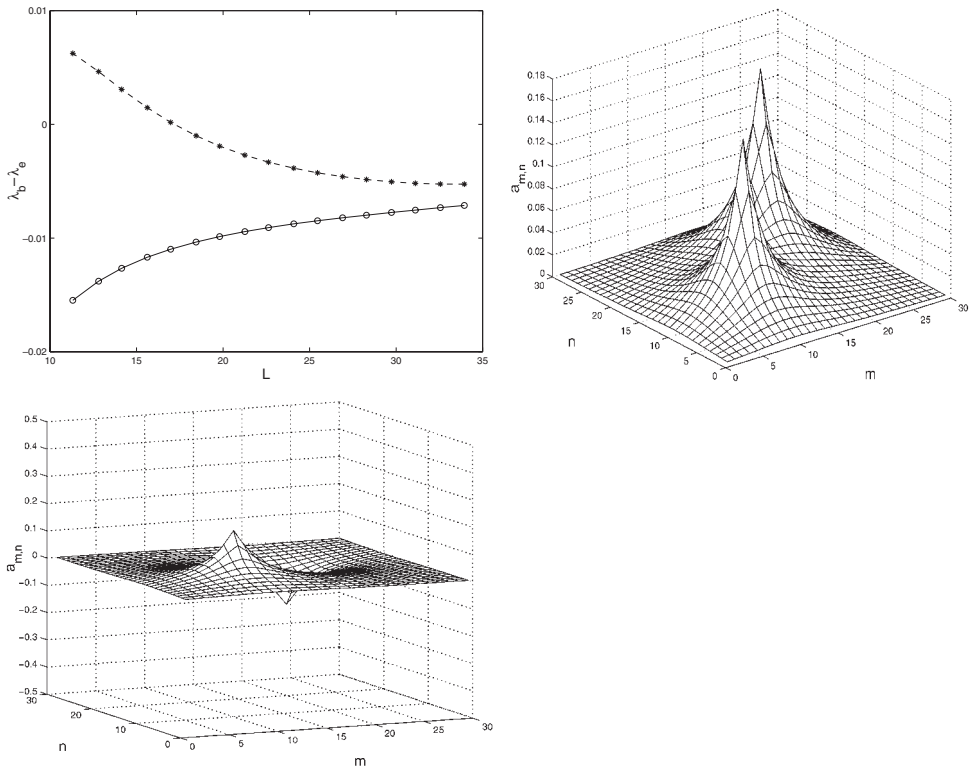

Figure 4. The (almost symmetric) variation of the two pairs of eigenvalues bifurcating from the bottom edge of the phonon band, as a function of the distance between the pulses (top-left panel). The bifurcating eigenvalues λ_b are shown with respect to the band edge $\lambda_e = |\Lambda|$; therefore, zero-crossing by one of the two eigenvalues shown here means that it returns to the phonon band. Numerical-data points for the two eigenvalues are shown by circles and stars, respectively, while the curves (solid and dashed) just connect the points to help follow systematic evolution of the eigenvalues. The top-right and bottom panels show a typical set of the corresponding eigenfunctions (the top-right panel for the smaller pair of the eigenvalues—shown by circles in the top-left panel—and the bottom panel for the larger pair of eigenvalues—shown by stars in the top-left panel). Shown is $a_{m,n}$; $b^{\star}_{m,n}$ demonstrates a similar behaviour.

- The exponential smallness of the interaction effects, expected in the case of the large separation between the pulses, is *not* obvious in the variation of these eigenvalues with respect to L.

To further probe the particle-like nature of the interaction, and also to ensure that (stable) bound states consisting of more than two pulses exist, we have performed the following *triangle* numerical experiment: three pulses were placed along a diagonal of the lattice. As is obvious from the previous results for the interaction of two pulses in 2D, as well as is suggested by the 1D DNLS models [27, 28], only . . . –up–down–up–down–. . . multipulse arrays, with the phase difference π between adjacent pulses, can be stable. Also, since we now have three pulses, we will have two small interaction-generated eigenvalues (more generally, for N -pulse configurations, $N-1$ such eigenvalues must be present). A stable three-pulse configuration is shown in figure 5. The left panel shows the configuration itself, while the right one demonstrates the results of the linear-stability analysis, with the inset clearly showing the presence of two interaction-induced eigenvalues in the neighbourhood of the origin of the complex λ plane.

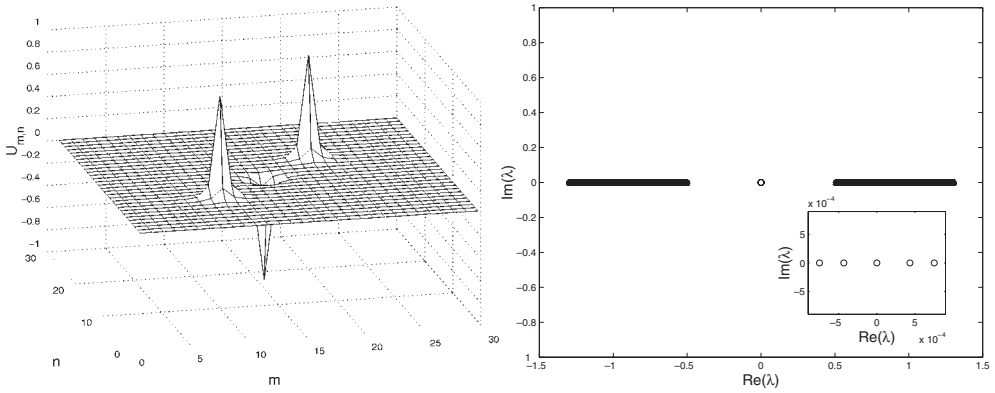

Figure 5. The triangle experiment: the straight configuration (i.e. $\theta = 180^\circ$) (left panel), and the corresponding eigenvalues (right panel). The inset clearly indicates the presence of two interaction-generated eigenvalues.

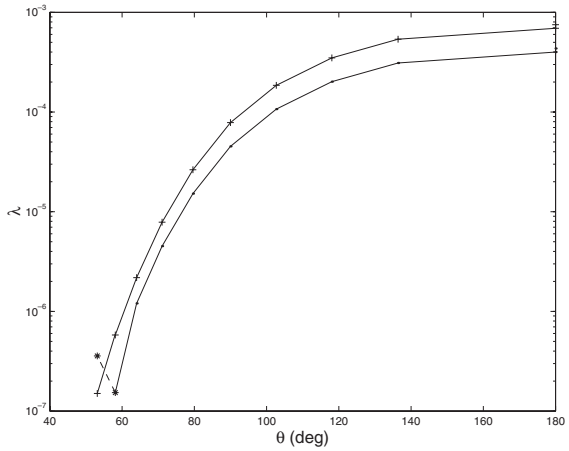

Figure 6. The triangle experiment: two interaction-generated eigenvalues versus the angle between the directions from the centre of the middle 'down' pulse to two 'up' pulses at the edges. Initially (for $\theta = 180^\circ$, see the previous figure), the pulses are aligned along a lattice diagonal. Gradually, the middle pulse is moved along the perpendicular diagonal, hence a triangle is formed. The values of the first eigenvalue are shown by dots connected by the solid line if they are real (i.e. stable), and by stars connected by the dashed line if they are imaginary (i.e. unstable). The second interaction-generated eigenvalue is always stable in the case considered, and it is shown by the plus symbols also connected by the solid curve. As remarked in the text, as soon as the triangle becomes equilateral, the configuration becomes unstable, as the 'up–up' destabilizing interaction overcomes the stabilization effect of the 'up–down' interactions.

We follow the behaviour of these two interaction eigenmodes as a function of the angle (starting from 180° downwards) of the triangle formed when moving the intermediate pulse down along the diagonal which is perpendicular to the one along which the three pulses were originally aligned. The variation of the interaction eigenvalues is shown in figure 6. A noteworthy effect is that the leading eigenvalue becomes unstable *immediately* as the triangle becomes equilateral. This is a strikingly straightforward demonstration of the particle-like nature of the interaction characteristics between the pulses (even in a strongly discrete case—in this example, $\Lambda = -0.5$ and $C = 0.1$, i.e. $h = \sqrt{10}$), as it shows that, as soon as the

destabilizing interaction of the 'up–up' pair of the pulses overcomes the stabilizing effect of the 'up–down' interactions (the distance between the unipolar pulses is smaller than that between the opposite-polarity ones if $\theta < 60^\circ$), the instability sets in.

4. Bound states involving vortex solitons

Recently, stable solitary waves with an intrinsic vorticity in the DNLS system were constructed in [26]. This was accomplished by constructing a discretized configuration in which the field pattern mimicked the dependence on the angular variable $\sim \exp(\mathrm{i}S\theta)$, characteristic of solitons with spin S in continuum models [50, 51]. In particular, this implies that the angular dependences of $\mathrm{Re}\, U_{m,n}$ and $\mathrm{Im}\, U_{m,n}$ resemble, respectively, $\cos(S\theta)$ and $\sin(S\theta)$. Hence the real part of the discrete two-dimensional stationary field should be odd in x, while the imaginary part should be odd in y. Following these expected symmetries, a *dual-twisted* ansatz, in which $\mathrm{Re}\, U_{m,n} = -\mathrm{Im}\, U_{-m,n}$ and $\mathrm{Im}\, U_{m,n} = -\mathrm{Im}\, U_{m,-n}$ (inspired by the 'twisted localized modes' recently found in the 1D DNLS model [34–37]), was used as a starting point for the Newton iteration scheme that had converged to a solution of equation (2.3) representing the discrete localized ('bright', in terms of nonlinear optics [50, 51]) vortex solution with $S = 1$. Direct dynamical tests have further demonstrated that the localized discrete vortex with $S = 1$ in the 2D DNLS model can be *stable* (vortices with $S > 1$ were also obtained, but they were found to be unstable). Naturally, as it is discussed below (and also in [26]), the stability is true only for weak coupling (i.e. small values of C).

Two drastic differences of the localized vortices in the DNLS model from their counterparts in various continuum models should be stressed. First, the axial symmetry of the continuous 2D NLS equation is broken in the discrete model, hence the vorticity is an intrinsic characteristic of the 2D discrete soliton which *cannot* be considered as an obvious topological invariant. Second, *all the vortices* are unstable not only in the continuum 2D NLS model, where the instability is a straightforward consequence of the fact that this model is subject to the (weak) wave collapse, but also in most other continuum models. For instance, they are strongly unstable against azimuthal perturbations in the model with the quadratic nonlinearity [50], where the collapse is absent, and zero-vorticity solitons are perfectly stable (very recently, the first example of stable localized vortices, alias *vortex rings*, with $S = 1$ and 2, has been found in a continuum model combining the quadratic and self-*defocusing* cubic nonlinearities [51]). Therefore, the existence of stable vortices in the DNLS lattice is an important property, and investigation of complexes involving these vortices, which is the subject of this section, is an interesting problem.

The main finding, produced by means of the Newton iterations followed by linear stability analysis, and finally confirmed by direct numerical integration of the full equation (2.1), is that bound states of $S = 0$ and 1 discrete solitons do exist, and they *can be* stable within the stability range of the isolated $S = 1$ discrete vortex solitons, i.e. for $C < C_{\mathrm{cr}}^{(1)} \approx 0.13$ (the $S = 0$ soliton is stable in its own region, $C < C_{\mathrm{cr}}^{(0)} \approx 0.32$) [26]. An example of the stable bound state of $S = 0$ and 1 solitons is shown in figure 7 in the top-left panel, while its linear stability is illustrated by the top-right panel.

The eigenvalue pair closest to the origin of the spectral plane corresponds to an interaction-generated eigenmode. The left and right bottom panels show, respectively, the real and imaginary components of the stationary field $U_{m,n}$. Such configurations exist when the distances between the $S = 0$ and the 1 solitons are about 3–5 sites or more (in the range of the coupling-constant values considered here, where the $S = 1$ pulse is linearly stable). In fact, even when instabilities arise for such values of the distance and coupling constant, they are *extremely weak* (typically at the level of numerical precision), hence they may be relevant only to much larger timescales than those considered here.

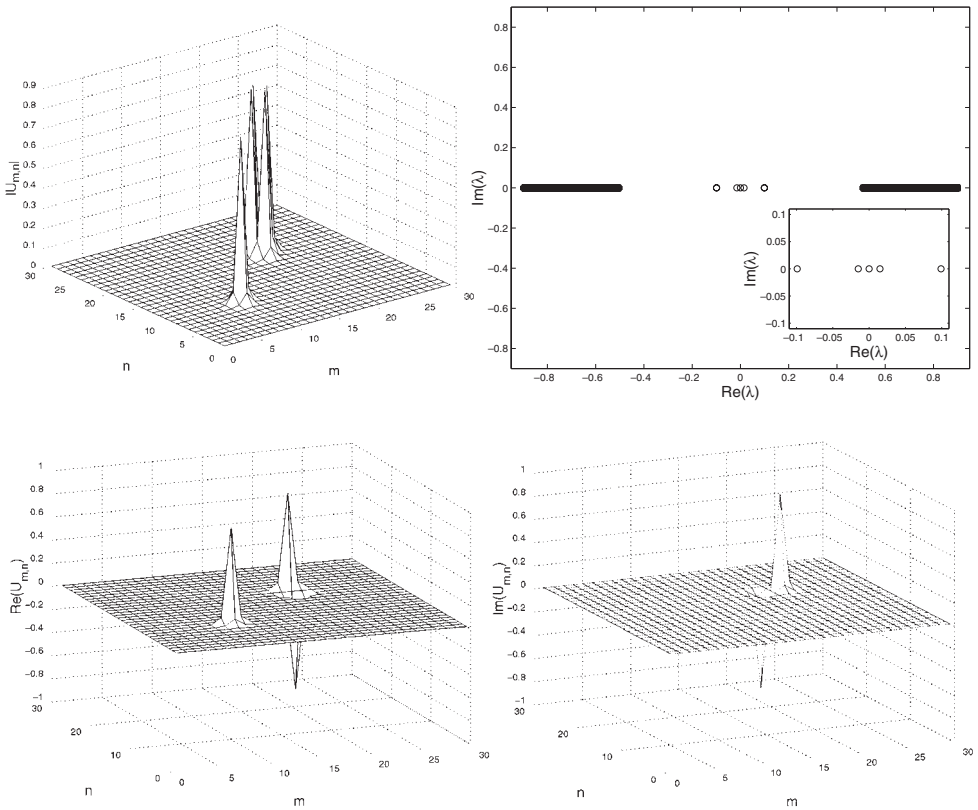

Figure 7. An $S = 0$–1 bound state. The absolute value of the corresponding solution to equations (2.3) is shown in the top-left panel. The results of linear stability analysis indicating the absence of unstable eigenmodes are shown in the top-right panel. The real and imaginary parts of the solution are shown in the bottom-left and bottom-right panels, respectively.

A bound state of two $S = 1$ solitons is shown in figure 8. The top-right panel again illustrates the linear stability, while the bottom panels show the real and imaginary parts of the stationary field. A novel result is that the bound state of two identical $S = 1$ vortex solitons with the zero phase difference (as those shown in figure 8) are *stable*, in contrast to what is the case for the $S = 0$ solitons (recall they must have the phase difference π to form a stable bound state). A qualitative explanation to this difference is suggested by the analogy to the 1D constituents of the vortices. In particular, the configurations of the real and imaginary parts of the stationary field corresponding to the bound state (shown in the bottom panels of figure 8) are such that the 'down' pulses contained in them are screening the destabilizing interaction between the 'up' pulses, and vice versa. The same argument can be used to justify the stability of configurations consisting of two π out of phase $S = 1$ modes. We have found that a minimum relative distance, approximately the same as in the case of the ($S = 0$–1) BS, is necessary for the formation of the BSs of two $S = 1$ solitons is also required here. For distances larger than this minimum distance, such configurations were typically found to be stable.

Finally, concerning the interaction-generated eigenmodes of such bound states, we will only present some preliminary conclusions here. A problem in the study of these modes is that, due to the larger effective size of the $S = 1$ solitons, it is harder to accurately analyse

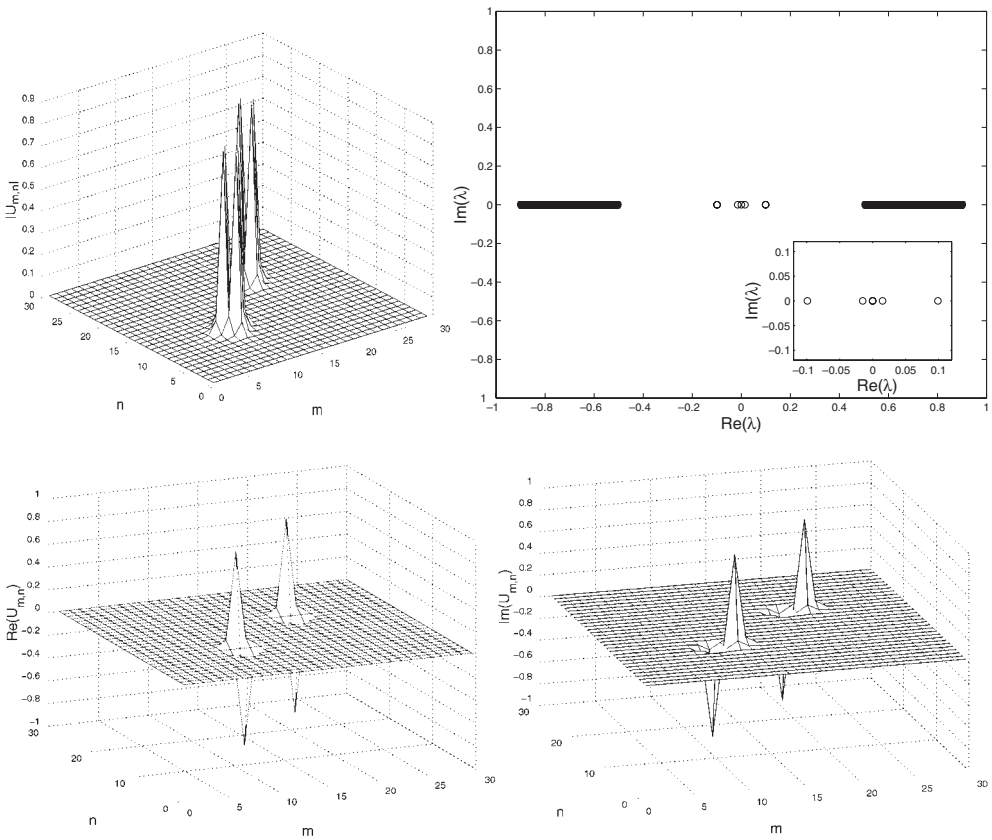

Figure 8. The same as in figure 7 for a bound state of two $S = 1$ discrete vortex solitons.

the dependence of the interaction-generated eigenvalues on the distance between the solitons, especially in the case of two $S = 1$ vortices. For this reason, we will not deal with the latter case, for which there is a direct analytical prediction of the stability of the bound state with zero phase difference, and instability of the state with phase difference of π, following from the quasi-continuum approximation [33]. We therefore only consider the bound state of the $S = 0$ and 1 solitons. With the change of the distance between them, a weak, angle-dependent variation of the interaction-generated eigenvalue was observed, which is detailed in table1. An additional problem that hinders the systematic observation of such eigenvalues is the fact that the bound states in question exist only for small values of the coupling constant, $C < C_{\rm cr}^{(1)}$, at which the $S = 1$ soliton is stable by itself.

5. Conclusion

In this work we have addressed, analytically and numerically, the problem of formation of multi-pulse bound states in 2D dynamical lattices of the DNLS type. This extends previous results for the formation of isolated pulses in such media, and the results regarding the formation of multi-soliton bound states in 1D lattices. Our essential conclusions are that such stable bound states of two or more zero-spin pulses exist indeed, and stable two-soliton bound states with one or both solitons having spin $S = 1$ are also possible. Another noteworthy result is the

Table 1. Variation of the interaction-generated eigenvalue of the ($S = 0$–1) bound state[a].

(n_1, m_1)	(n_2, m_2)	$\lambda \times 10^9$
(10, 10)	(17, 17)	0.207(919)
(10, 11)	(17, 17)	0.331(314)
(10, 12)	(17, 17)	0.136(507)
(11, 11)	(17, 17)	0.280(401)
(11, 12)	(17, 17)	0.431(588)

[a] The coordinates (n_1, m_1) of the centre of the $S = 0$ soliton are varied, while the position (n_2, m_2) of the $S = 1$ soliton is kept fixed. The third column shows the interaction-generated eigenvalue (the last three digits in the parenthesis in this column indicate the next decimal digits in the value of λ). The data support a (preliminary, for reasons explained in the text) conclusion that the interaction-generated eigenvalue varies weakly with the separation between the two solitons constituting the bound state. Notice also that the non-monotonic dependence of the eigenvalue versus the separation suggests that the eigenvalue is sensitive to the natural anisotropy of the lattice model.

elucidation of the particle-like character of the interaction between $S = 0$ pulses, even in the strongly discrete case. A consequence of the 2D character of the soliton–soliton interaction in the system is the presence of the power-law pre-exponential multiplier in the effective interaction potential (2.14), which affects the estimate of the interaction-generated stability eigenvalue (3.20) of the bound state. This prediction has been found to be in very good agreement with direct numerical results. Other numerical experiments, such as those with the triangle configuration, were also performed, providing additional insight into the formation, stability and behaviour of multi-pulse bound states in the 2D nonlinear lattices.

Due to the stabilizing effect of the discreteness, the DNLS model with the cubic nonlinearity, which is a generic dynamical model, and also has direct applications to various physical systems (for instance, to the light propagation in a bundle of nonlinear optical fibres) provides an ideal probing ground for the generation of various multi-pulse coherent patterns and study of their properties and interactions.

Acknowledgments

This research was, in a part, supported by the US Department of Energy, under contract W-7405-ENG-36, and by the Binational (US-Israel) Science Foundation, through grant no 1999459. BAM appreciates hospitality of the Center for Nonlinear Studies and Theoretical Division at the Los Alamos National Laboratory.

References

[1] Peyrard M and Bishop A R 1989 *Phys. Rev. Lett.* **62** 2755
[2] Kopidakis G and Aubry S 1999 *Physica* D **130** 155
[3] Swanson B L *et al* 1999 *Phys. Rev. Lett.* **82** 3288
[4] Christodoulides D N and Joseph R I 1988 *Opt. Lett.* **13** 794
[5] Newell A C and Moloney J V 1992 *Advanced Topics in the Interdisciplinary Mathematical Sciences* (New York: Addison-Wesley)
[6] Agrawal G P 1988 *Nonlinear Fiber Optics* (New York: Academic)
[7] Aceves A, De Angelis C, Trillo S and Wabnitz S 1994 *Opt. Lett.* **19** 332
Aceves A, De Angelis C, Luther G G and Rubenchik A M 1994 *Opt. Lett.* **19** 1186
Aceves A *et al* 1995 *Phys. Rev. Lett.* **75** 73
Aceves A *et al* 1996 *Phys. Rev.* E **53** 1172
Aceves A and Santagiustina M 1997 *Phys. Rev.* E **56** 1113
[8] Campa A and Giasanti A 1998 *Preprint* physics/9802043

[9] Morandotti R *et al* 1999 *Phys. Rev. Lett.* **83** 2726
[10] Eisenberg H *et al* 1998 *Phys. Rev. Lett.* **81** 3383
[11] See, e.g. Flach S and MacKay R S (ed) 1998 *Physica* D **119** a special issue on discrete breathers
[12] MacKay R S and Aubry S 1994 *Nonlinearity* **7** 1623
[13] Fisher F 1993 *Ann. Phys., Lpz.* **2** 296
[14] Takeno S 1992 *J. Phys. Soc. Japan* **61** 2821
Flach S, Kladko K and Takeno S 1997 *Phys. Rev. Lett.* **4838** 4838
[15] Burlakov V M, Kiselev S A and Pyrkov V N 1990 *Phys. Rev.* B **42** 4921
Flach S, Kladko K and Willis C R 1994 *Phys. Rev.* E **50** 2293
Tamga J M, Remoissenet M and Pouget J 1995 *Phys. Rev. Lett.* **75** 357
[16] Cretegny T and Aubry S 1997 *Phys. Rev.* B **55** R11 929
Cretegny T and Aubry S 1998 *Physica* D **113** 162
[17] Pouget J, Remoissenet M and Tamga J M 1993 *Phys. Rev.* B **47** 14 866
[18] Flach S, Kladko K and MacKay R S 1997 *Phys. Rev. Lett.* **78** 1207
[19] Kevrekidis P G, Rasmussen K Ø and Bishop A R 2000 *Phys. Rev.* E **61** 2006
[20] Kevrekidis P G, Rasmussen K Ø and Bishop A R 2000 *Phys. Rev.* E **61** 4652
[21] Christiansen P L, Gaididei Yu B, Rasmussen K Ø, Mezentsev V K and Juul Rasmussen J 1996 *Phys. Rev.* B **54** 900
[22] Mezentsev V K, Musher S L, Ryzhekova I V and Turitsyn S K 1994 *JETP Lett.* **60** 829
[23] Laedke E W, Spatschek K H, Mezentsev V K, Musher S L, Ryzhekova I V and Turitsyn S K 1995 *JETP Lett.* **62** 677
[24] Johansson M, Aubry S, Gaididei Yu B, Christiansen P L and Rasmussen K Ø 1998 *Physica* D **119** 115
[25] Bonart D, Mayer A P and Schröder U 1995 *Phys. Rev. Lett.* **75** 870
Kiselev S A and Sievers A J 1997 *Phys. Rev.* B **55** 5755
[26] Malomed B A and Kevrekidis P G 2001 *Phys. Rev.* E **64** 026601
[27] Kapitula T, Kevrekidis P G and Malomed B A 2001 *Phys. Rev.* E **63** 036604
[28] Kevrekidis P G 2001 *Phys. Rev.* E **64** 026611
[29] Weinstein M I 1999 *Nonlinearity* **12** 673
[30] Johansson M and Aubry S 2000 *Phys. Rev.* E **61** 5864
[31] Kevrekidis P G, Saxena A B and Bishop A R 2001 *Phys. Rev.* E **64** 026613
[32] Aubry S 1997 *Physica* D **103** 201
[33] Malomed B A 1998 *Phys. Rev.* E **58** 7928–33
[34] Laedke E W, Kluth O and Spatschek K H 1996 *Phys. Rev.* E **54** 4299
[35] Johansson M and Aubry S 1997 *Nonlinearity* **10** 1151
[36] Darmanyan S, Kobyakov A and Lederer F 1998 *Sov. Phys.–JETP* **86** 318
[37] Kevrekidis P G, Bishop A R and Rasmussen K Ø 2001 *Phys. Rev.* E **63** 036603
[38] Kevrekidis P G, Malomed B A, Bishop A R and Frantzeskakis D J 2001 Localized vortices with a semi-integer charge in dynamical lattices, to be published
[39] Carr J and Eilbeck J C 1985 *Phys. Lett.* A **109** 201
[40] Eilbeck J C, Lomdahl P S and Scott A C 1985 *Physica* D **16** 318
[41] Morgante A M, Johansson M, Kopidakis G and Aubry S 2000 *Phys. Rev. Lett.* **85** 550
[42] Johansson M and Kivshar Yu S 1999 *Phys. Rev. Lett.* **82** 85
[43] Kevrekidis P G and Weinstein M I 2001 Breathers on a background: periodic and quasiperiodic solutions of extended discrete nonlinear wave systems, submitted
[44] Braun O M, Kivshar Yu S and Peyrard M 1997 *Phys. Rev.* E **56** 6050
[45] Kivshar Yu S, Pelinovsky D E, Cretegny T and Peyrard M 1998 *Phys. Rev. Lett.* **80** 5032
[46] Kevrekidis P G and Jones C K R T 2000 *Phys. Rev.* E **61** 3114
[47] Kapitula T, Kevrekidis P G and Jones C K R T 2001 *Phys. Rev.* E **63** 036602
[48] Kapitula T and Kevrekidis P G 2001 *Nonlinearity* **14** 533
[49] Marin J L and Aubry S 1998 *Physica* D **119** 163
[50] Firth W J and Skryabin D V 1997 *Phys. Rev. Lett.* **79** 2450
Petrov D V and Torner L 1997 *Opt. Quantum Electron.* **29** 1037
[51] Towers I, Buryak A V, Sammut R A and Malomed B A *Phys. Rev.* E **63** 055601(R)